RASĀYAN *J. Chem.*
Vol. 18 | No. 4 | 2506-2520 | October-December | 2025
ISSN: 0974-1496 | e-ISSN: 0976-0083 | CODEN: RJCABP
http://www.rasayanjournal.com
http://www.rasayanjournal.co.in

SUSTAINABLE BIOSORPTION OF LEAD(II)IONS FROM AQUEOUS SOLUTIONS BY *Nymphaea pubescens* STEM: A COMPREHENSIVE BATCH STUDY

K. Talukdar[1,2], N. Sarma[3,4], S. Rabha[3,4], B. Devi[3,1], M. Goswami[3,5], E. Das[3,4] and A. Devi[3,4,✉]

[1]Department of Chemistry, Gauhati University, Guwahati-781014, (Assam) India
[2]Department of Chemistry, Abhayapuri College, Abhayapuri-783384, (Assam) India
[3]Environmental Chemistry Laboratory, Resource Management and Environmental Section, Life Science Division, Institute of Advanced Study in Science and Technology (IASST), Guwahati-781035, (Assam) India
[4]Academy of Scientific and Innovative Research (AcSIR), Ghaziabad-201002, India
[5]Department of Environmental Science, Gauhati University, Guwahati-781014, (Assam) India
✉Corresponding author: deviarundh2@yahoo.co.in

ABSTRACT

The adsorption of Lead(II)ions on the stem of *Nymphaea pubescens* (*N. pubescens*), a reusable plant material, has been studied using a variety of parameters, including pH, contact time, adsorbent quantities, Lead(II)ion concentration, and temperature, by the batch equilibrium technique. The study proved that *N. pubescens* was highly efficient in removing Lead(II)ions at pH 7 and 323K temperature with a removal efficiency of 99.8%, making it a promising environmentally conscious adsorption material for heavy-metal contamination. The Langmuir isotherm and Elovich kinetic models more closely fit the experimental equilibrium data. Lead (II) ions highlighted an optimal adsorption capability (q_{max}) of 50.51 mg/g at 323K on the adsorbent. The study of thermodynamic variables demonstrated that the adsorption is spontaneous, feasible, and endothermic in nature with a positive ΔH° and negative ΔG° value. In accordance with the desorption analysis, the biosorbent can be reused for as many as three cycles. The present study holds considerable environmental and scientific significance in addressing the critical issue of heavy metal contamination in water, particularly lead(II), which poses serious health risks and ecological damage even at low concentrations. The key contributions and implications of the study are the development of a low-cost and environmentally sound adsorbent, comprehensive characterization and modelling, thermodynamic validation of feasibility and spontaneity, and the possibility of waste valorisation and reutilization. This work lays the groundwork for future studies involving real wastewater treatment, multi-metal systems, column studies, and commercial-scale implementation, contributing to ongoing efforts in sustainable environmental remediation.

Keywords: Adsorption, Nymphaea *pubescens* Stem, Lead(II), Kinetics, Isotherm, Thermodynamics, Regeneration.
RASĀYAN *J. Chem.*, Vol. 18, No.4, 2025

INTRODUCTION

Were you intrigued to learn that even the most minute amounts of harmful metals in water can trigger extremely serious health issues, for instance, neurological illnesses, damage to the liver, and malignancies?[1] The elevated concentrations of industrial emissions, most notably heavy metal elements, in water bodies have been identified as an urgent ecological problem over the past decades, owing to the proliferation of civilization and the global economy.[2] Heavy metals, a class of pervasive toxic substances in the environment, can be bioaccumulated or intensified in food systems and can be harmful to human health. Since heavy metals are widely employed in human-induced processes such as mineral extraction, production, agriculture (fertilizer and insect repellent), and waste expulsion, heavy metal contamination of aquatic systems has emerged as a worldwide environmental concern. Lead, copper, arsenic, mercury, zinc, and cadmium are among the heavy metals that are extremely harmful when assimilated by the human body. Lead (Pb) is the most prevalent poisonous metal that has been associated with cancer, nervous system malfunction, chronic intoxication, and other issues.[3] Lead is an enzyme inhibitor and a

http://doi.org/10.31788/RJC.2025.1849404

general metabolic toxin. Infants and kids might suffer mental impairment and lifelong brain damage as consequences. The removal of these hazardous metals from watersheds and wastewaters requires immediate attention because lead may substitute for calcium in the bone and generate sites for prolonged release. According to the Environmental Protection Agency, the maximum amount of lead that can be found in wastewater is 0.1 mg/L, whereas the maximum quantity that can be found in drinking water is 0.05 mg/L.[4] The World Health Organization has established an optimal lead level in drinking water at 0.01 mg/L (WHO, 2003). Since international regulations and regulatory bodies are growing more stringent in their enforcement of effluent standards, wastewater treatment is consequently crucial. The significant operational costs incurred by eliminating contaminants, however, may make it challenging for most new companies to adhere to these pollution prevention demands.[5] Heavy metal-contaminated waste streams and soil may usually be detoxified via innovative technologies like ion exchange, membrane filtration, precipitation, reverse osmosis, solidification/stabilization, and carbon adsorption. Despite the expense of substrate substances and regeneration being a restraining issue, sorbent-based techniques are possibly the most widely employed. Therefore, a great deal of emphasis has been put on characterizing the sorption characteristics of cost-effective substitutes, which include dead biomass and natural adsorbent materials.[6] The processes of adsorption occur at the surface and are brought on by chemical or physical forces. The key factors governing the adsorbate absorption rate are adsorption kinetics and isotherms, which establish the adsorption variables and exhibit the adsorbent's adsorption efficacy. The pseudo-first order, pseudo-second order, and Elovich models, as well as the Langmuir, Freundlich, Temkin, and Toth models, are predominant kinetic and isotherm models that explain the adsorption process.[7] We looked at the impacts of temperature, pH, concentration, and contact time. The effects of the solution's pH (4–7), biosorbent dose (0.6–2.2 g/L), contact time (20–180 min), and initial metal ion concentration (25–100 mg/L) were all examined in batch adsorption studies conducted at temperature of 30–5. From the adsorption measurements, the kinetic parameters and adsorption isotherm were assessed. Assam is rich in wetlands, covering an area of 1,400 square kilometers with around 3,000 large and minor wetlands distributed throughout the state. This work aims to discover a low-cost, sustainable adsorbent; to obtain high removal efficiency under mild conditions; to investigate the potential for reusability of *N. pubescens,* which was collected from wetlands of Assam; and to lay the foundation for future research and scale-up. Due to a dearth of knowledge about its adsorption capabilities, this plentiful and renewable plant material was selected as an adsorbent. The study suggests using a cost-effective and environmentally friendly approach that does not require chemical activation to remove lead ions from aqueous solutions and to achieve better water quality by encouraging the valorization of biomass waste, which directly promotes SDG-6 (Clean Water and Sanitation). Although the study demonstrates that the *Nymphaea pubescens* stem is an efficient and reusable biosorbent to eliminate Lead(II)ions from aqueous solutions under controlled laboratory settings, several key gaps remain unaddressed, such as real-world application and wastewater complexity, long-term reusability and regeneration efficiency, scale-up and process optimization, economic and environmental assessment, and mechanistic insights at the molecular level.

EXPERIMENTAL

Chemicals

Lead nitrate ($Pb(NO_3)_2$) was utilized for preparing a stock solution of 1000 mg/L concentration. By diluting the stock solution with Mili-Q water, the other solutions having concentrations of 25 mg/L, 50 mg/L, 75 mg/L, and 100 mg/L were prepared. All the chemicals utilized throughout the laboratory experiment were analytically pure and were purchased from Sigma Aldrich.

Preparation of Biosorbent

Fresh *Nymphaea pubescen*s were collected from wetlands of Assam, of which only the stem is used for the experiment. Following multiple washes with deionized water, the collected stems were dried. Afterwards, the dried leaves are sieved to a particle size of 75-200 nm.[4] The produced powder was washed with distilled water until colorless and then dried in sunlight before being put in a hot air oven at 40℃. After that the powder was ground by an electric mixer and then kept in a clean glass bottle.

Biosorbent Characterization

An FT-IR spectrophotometer was employed to determine the functional groups that exist on the biosorbent. A TGA analyzer was used to determine the thermal stability of the biosorbent. Zeta potential was used to examine the surface charge. FESEM was done both before and after adsorption to know the morphology of the biosorbent. To validate the adsorption of Lead(II)on the biosorbent, EDX analysis was carried out. The CHNS investigation was carried out with a Thermo FLASH Smart Analyzer to determine the elemental composition and its percentage in the biosorbent. An X-ray photoelectron spectrophotometer was used to analyze surface chemical states of C1S, O1S, and N1S XPS spectra.

Batch Study of Lead Adsorption

Batch experiments were conducted in 100 ml Erlenmeyer flasks in a thermostatic orbital shaker. For the batch study, biosorbent doses of 0.6-2.2 g/L were taken, and experiments were carried out at an agitation speed of 150 rpm at different pH levels from 4 to 7. The experiments were done to explicate the optimum conditions of pH and biosorbent dose. The optimum pH and biosorbent dose were found to be 7 and 2.2 g/L, respectively. Then batch experiments were carried out using this optimum pH and adsorbent dose at three different temperatures (30℃, 40℃, and 50℃) for 20 to 120 minutes. Metal solutions from 25 to 100 mg/L were prepared to analyze how the concentration of metal ions affected adsorption. As part of pH investigations, the pH levels were continuously monitored after introducing 0.1 N HCl or 0.1 N NaOH into the Lead(II)solution. All the solutions were filtered by using 42 Whatman filter paper, and the obtained filtrate was subsequently examined using an atomic absorption spectrophotometer (AAS, AA7000, Shimadzu) to find out the Lead(II)concentration.

The adsorption capacity and the removal percentage of lead (II) by *N. pubescens* stem have been estimated by applying the subsequent equations.

$$q_t = \left(\frac{C_0 - C_e}{m}\right) v \quad (1)$$

$$\text{Removal percentage (\%) of Lead(II)} = \frac{C_0 - C_e}{C_0} \times 100 \quad (2)$$

Here, q_t is the adsorption capacity (mg/g), C_0 (mg/L) is the initial concentration, and Ce (mg/L) is the equilibrium concentration of Lead(II)in solution. V(L) and m (mg) indicate the volume of the solution and the weight of the biosorbent, respectively.

Desorption and Regeneration Study

The hydrochloric acid (HCl) solutions having different concentrations were used to desorb lead from the adsorbent. Experiments were done using 0.1, 0.5, 0.75, and 1 M HCl to assess the reuse efficiency of the adsorbent. The adsorbent loaded with Pb (II) ions was dried at 40℃ and then treated with 100 mL of HCl solutions of each concentration for 3 hours. The regenerated adsorbent substance was employed for the biosorption of Lead(II)in solution. Spectrophotometric techniques were used for assessing the desorbed Lead(II)ions in the acidic solutions.

RESULTS AND DISCUSSION

FTIR Analysis

FTIR was implemented to find out the functional groups that are responsible for metal adsorption.[8] The peaks attributed to functional groups of *N. pubescens* stem before and after adsorption of Pb (II) are shown in Fig.-1a. The adsorption peak at 3294 cm^{-1}, which is responsible for O-H stretching of water or alcohol, shifted to 3381 cm^{-1} after adsorption.[9] Methyl groups exhibit a peak at 2919 cm^{-1} due to C-H stretching and change the position to 2923 cm^{-1} after adsorption. The C=O functional group present on the biosorbent is confirmed by a peak at 1622 cm^{-1}, which is shifted to 1632 cm^{-1} after adsorption. A shift was noticed from 1425 to 1450 cm^{-1} after adsorption, which is responsible for the C-O stretching of the carboxylic or carbonate group. This shifting affirmed that functional groups participate in the binding of lead (II) ions on the surface of the biosorbent.[10]

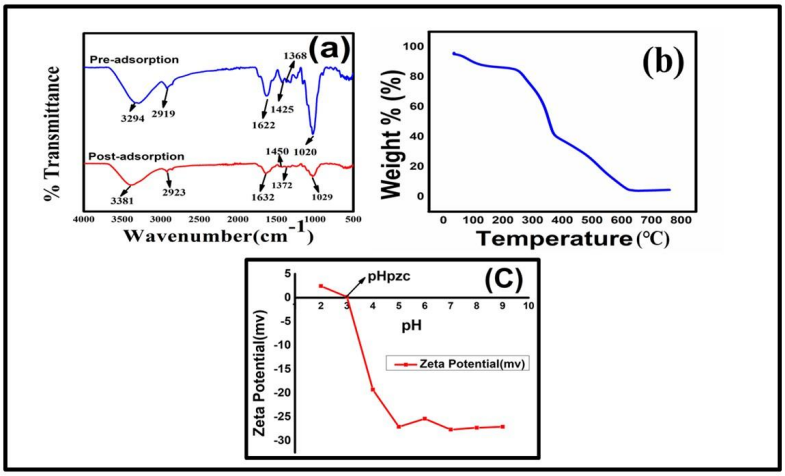

Fig.-1: FTIR spectra of *N. pubescens* Stem (a) Pre-Adsorption and Post-Adsorption, (b) TGA Study of *N. pubescens* Stem, and (c) Zeta Potential Analysis of *N. pubescens* Stem

TGA Analysis

Degradation of three phases was seen in thermogravimetric analysis, which is shown in Fig.-1b. The first weight loss, which occurred from room temperature to 100°C, was 6.05%, which indicates loss of some volatile compounds, moisture, and release of some water molecules from the biosorbent. The second stage of weight loss occurs between 240 and 360°C, which was 36.06% due to the release of CO_2 , CO, H_2 , and CH_4 , and decomposition of hemicellulose and cellulose. 49.89% of weight loss occurs in the third stage, between 380°C and 660°C. This can be attributed to the decomposition of the cellulose and lignin of the biosorbent.[11]

Zeta Potential Study

Zeta potential analysis was used to determine the surface charge of *N. pubescens* stem within the pH range of 2 to 9. The findings established that at pH 2 and 3, the biosorbent's surface charge was positive and negative at a pH range from 4 to 9, as shown in Fig.-1c. Figure-1c showed that the adsorbent's zero-point charge (pH_{PZC}) lies around pH 2.9. The pHpzc is noteworthy since this value reveals the pH level at which the adsorbent's surface reaches neutral electrical charge.[12] The possible existence of carboxylates and phenolic hydroxyl functional groups might serve as contributing factors to the negative zeta potential charge. Heavy metal adsorption is aided by the biosorbent's negative charge. Therefore, it can be figured out that the electrostatic interaction of Lead(II)ions with the biosorbent's functional groups (negatively charged) is predominantly accountable for the biosorption of Lead(II)ions on *N. pubescens's* surface.

SEM and EDX Analysis

FESEM images of *N. pubescens* before and after adsorption of Pb were taken, and they revealed that before adsorption, the surface was rough and porous, as shown in Fig.-2a. After adsorption, the surface was covered by Pb(II) ions, and it became smooth, which is illustrated by Fig.-2b.[13]

The appearance of O and C peaks on EDX spectra reflects the availability of -COOH and O-H functional groups on the biosorbent. The elemental composition of carbon and oxygen was shown on the EDS spectra, Fig.-2c. In addition to this, Ca, Mg, Al, and Si are also present in smaller percentages.[11] The peak on EDX spectra after adsorption (Fig.-2d) asserted the biosorption of Pb on the adsorbent. [13]

Elemental Analysis

Elemental analysis was performed to analyse the adsorbent compositions. Table-1 shows the adsorbent's elemental composition both before and after adsorption, and it reveals that nitrogen has a minimal concentration compared to carbon and hydrogen.[14] After adsorption of Lead(II)ions, the quantity of carbon, hydrogen, and nitrogen decreases.

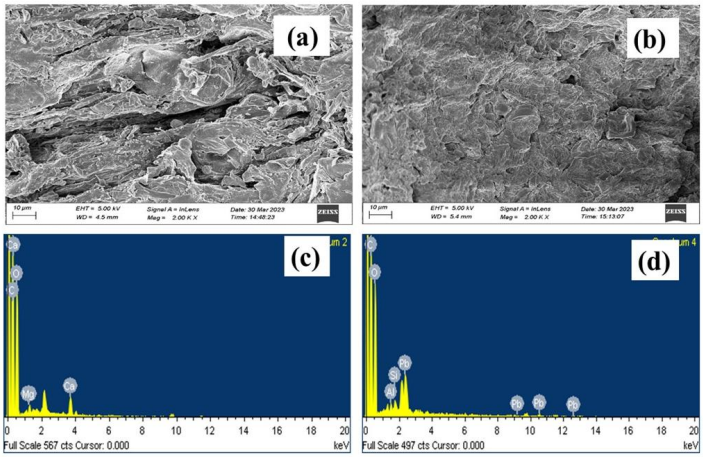

Fig.-2: SEM image of *N. pubescens* Stem (a) Pre-Adsorption and (b) Post-Adsorption, and EDX Spectra of *N. pubescens* Stem (c) Pre-Adsorption and (d) post-adsorption

It may be due to Lead(II)ions occupying the free space on the adsorbent's surface after adsorption and displacing the functional groups containing carbon and hydrogen, causing the apparent decrease in the percentage composition of the elements when considering the overall weight of the adsorbent before and after being loaded with lead ions.

Table-1: Elemental Analysis of *N. pubescens* Stem Powder

Element	Pre-adsorption (%)	Post-adsorption (%)
C	36.340	35.272
H	5.276	4.964
N	0.218	0.057

XPS Analysis

XPS was applied to look over the preceding relationship between the contaminants and functional groups of adsorbents to validate the results from FTIR spectrum analysis. By monitoring deviations in binding energies, the approach not only made it achievable to inspect the elements of carbon, oxygen, lead, and other constituents, but it also gave key details about variations in the chemical valence states. The biomaterial's XPS spectra study unambiguously shows that carbon and oxygen components are predominant in the surface of the adsorbent (wide scan spectra, Fig.-3a). These atoms are presumably accountable for the peaks of 287.2-284.8 eV (C1s) (Fig.-3b) and 533.00-532.56 eV (O1s) (Fig.-3c).[15-20] The tiny peak at 400.08-399.86 eV, as represented in Fig.-3d states the presence of nitrogen in the biomaterial.[21,22] The nitrogen concentration ascended, and the nitrogen peaks turned out notably more noticeable in the XPS spectra following the Lead(II)ion adsorption. The adsorbent-adsorbate interaction was further illustrated by the spotting of a small lead peak right after the adsorption of lead metal ions (Fig.-4a). Before the Lead(II)ion adsorption, the C 1s peaks were investigated by XPS, shown in Fig.-3b, which discovered three confined peaks at 284.7 eV (denoting C–C/C = C bonds), 286.4 eV (an indication of C–O bonds), and 286.93 eV (which is connected with C = O bonds). These peaks changed to 284.8, 286.14, and 287.4 eV, respectively, soon after Lead(II)ions were added (Fig.-4c).[23] A significant modification in surface chemistry is detected by an alteration in peak locations. On the other hand, Fig. 4b provides evidence that Lead(II)ions emerge on the adsorbent surface as established by binding energy maxima at 138.94 and 143.85 eV for Pb 4f7/2 and Pb 4f5/2. The altered binding energy of O1s and N1s, as displayed in Fig.-4d and Fig.-4e after the adsorption of Lead(II)ions on the surface of *N. pubescens* stem, suggests that the functional groups present on the surface of the adsorbent build coordinate bonds with lead contaminants. The negatively charged carboxyl and hydroxyl groups present on the adsorbent's surface cause electrostatic attraction by attracting positively charged Lead(II)ions on the surface of the adsorbent.[14] The negatively charged carboxyl and hydroxyl groups present on the adsorbent's surface

cause electrostatic attraction by attracting positively charged Lead(II)ions on the surface of the adsorbent.[14]

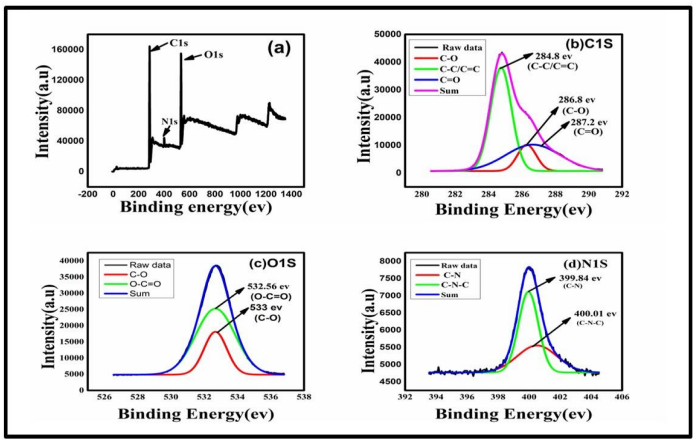

Fig.-3: XPS Analysis of *N. pubescens* Stem at Pre-Asdsorption of Lead(II)(a) Wide Scan XPS Spectra of Lead(II)(b) C1s Orbital XPS Spectra (c) O1s Orbital XPS Spectra (d) N1s Orbital XPS Spectra

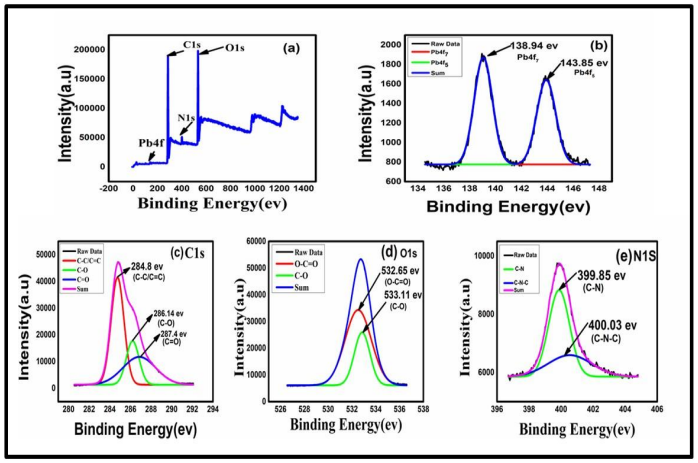

Fig.-4: XPS Analysis of *N. pubescens* Stem at Post-Adsorption of Lead(II)(a) Wide Scan XPS Spectra for Lead(II)(b) XPS Spectra for Pb 4f Orbital (c) XPS Spectra for C1s Orbital (d) XPS Spectra for O1s Orbital (e) XPS Spectra for N1s Orbital

Impact of Different Parameters on Biosorption

The effects of adsorbent dosage, contact time, pH, and metal ion concentration on the adsorption of Lead(II)ions on the surface of *N. pubescens* stem were explored using batch equilibrium tests.[24]

Impact of the pH

The adsorption process is profoundly impacted by the pH of the solution. A batch experiment was executed at a pH range of 4-7. After pH 7, solid precipitation of Pb $(OH)_2$, $Pb(OH)^+$, and $Pb(OH)_3$ was observed. So, the experiment was continued up to pH 7.[24.] At a lower pH 7, the concentration of protons is high, and it increases competition between hydrogen and metal ions for binding locations on the surface of the biosorbent.[12] As pH increases, the negatively charged hydroxyl and carboxylate functional groups attract the positively charged Pb (II) ions and thus enrich the adsorption.[25] Hence, it was observed that with increasing pH, adsorption increases, and maximum adsorption occurred at pH 7 (Fig.-5a).

Impact of the Contact Time

A batch experiment with respect to contact time was performed at room temperature. Initially, the adsorption was fast owing to the adsorbent's larger surface area, which is accessible at the onset of the adsorption process.[26]

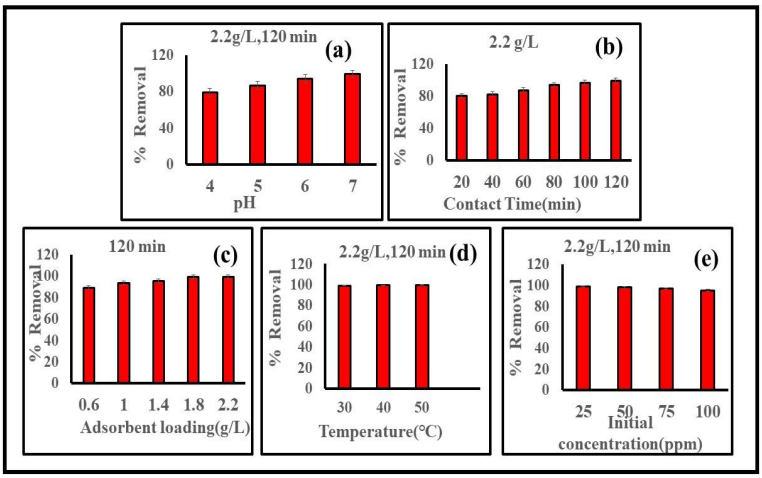

Fig.-5: The Impact of Different Factors on Lead(II) Removal by *N. pubescens* Stem
(a) Impact of pH, (b) Impact of Contact Time, (c) Impact of Biosorbent Dose, (d) Impact of Temperature, (e) Impact of Initial Metal Ion Concentration

Figure-5b displays that the removal capacity increases with increasing time. At 120 minutes, adsorption achieved equilibrium, after which the percentage of Lead(II)ions removed from the solution remains unchanged. This has been ascribed to the surface pores of the biosorbent, which may be clogged by lead ions, and it was challenging for further penetration inside the pores.[24] Hence, the most optimal contact time for every experiment was determined to be 120 minutes.[27]

Impact of the Adsorbent Loading

Biosorbent performs a vital function in the elimination of metal ions from aqueous solutions. It has been shown in Fig.-5c that with increasing the amount of biomass, the efficacy of % removal increases, but after attaining the saturation point, the % removal capacity decreases due to the assemblage of active areas on the biosorbent's surface.

Impact of the Temperature

In metal adsorption, temperature is the most significant parameter for energy-dependent mechanisms. As exhibited in Fig.-5d, lead ion adsorption utilizing *N. pubescens* stem is most appreciative at higher temperatures. As the temperature increases from 30℃ to 50℃, the adsorption of lead ions on *N. pubescens* stems increases, which denotes that adsorption is endothermic. At elevated temperatures, there are more binding sites of the adsorbent, which could be ascribed to the expansion of the pore diameter on the adsorbent's surface at higher temperatures.[27] Hence, the optimum temperature for further batch experiments was considered to be 323 K for all the concentrations.

Impact of the Initial Metal Ion Concentration

The impact of metal ion concentration on the elimination of lead ions was studied at a concentration range of 25-100 mg/L in a batch experiment. It has been seen from the investigation that with increasing initial concentration of Pb (II) from 25 to 100 mg/L, the % removal of Lead(II)ions decreases (Fig.-5e).[24] This seems to be due to the limited number of active locations on the biosorbent's surface after reaching the saturation state. When metal ion concentration increases, the surface area of the biosorbent becomes less able to hold the excess metal ions from the solution.[4]

Study of the Kinetics of Adsorption

The adsorption kinetics of Lead(II)on the stem of *N. pubescens* were studied under previously optimized conditions. The rate of the biosorption process was inspected comprehensively by employing different kinetic models to determine the rate-controlling step and the mechanism involved in the adsorption of Lead(II)ions.[28] Kinetic models, such as Pseudo-first-order, Pseudo-second-order, and Elovich models, are used to understand the mechanism of the adsorption process.[29] The equations of these non-linear kinetic models are displayed in Table-2. The kinetics of adsorption was investigated at the contact time ranging

from 20 to 120 minutes for a Pb (II) solution of 25 mg/L.[12] The adsorption kinetics have been predicted using pseudo-first-order, pseudo-second-order, and Elovich models based on the experimental data, and the ability of the kinetics for adsorption was interpreted by non-linear plots of q_t vs t. The correlation coefficient, R^2, and theoretical adsorption capabilities derived from these plots were used to assess the various kinetic models, and findings are presented in Table-3. The findings demonstrated that the Elovich model matched the experimental data more accurately than the other models (Fig.-6a,b,c).[27,33] Since the Elovich kinetic model's correlation coefficient values (0.994-0.995) are greater than the Pseudo first-order (0.978-0.982) and Pseudo second-order (0.988-0.991) kinetic models, and it has less chi-square value, χ^2 (0.092-0.114), than the other two models (Pseudo first-order, χ^2 = 0.332-0.395, and pseudo-second-order, χ^2 = 0.169-0.204), so Elovich kinetic model is a better fit for illustrating the adsorption kinetics of the biosorbent derived from *N. pubescens* stem.[34] With the rise in the solution temperature from 30 to 50℃, the adsorption rate constant of the Elovich model increases from 75.94 to 209.46.[27.] Through a well-fitted Elovich model, the kinetic data from the experiments focused on how the chemical interactions among the Lead(II)ions and the biomaterial's active binding locations control the adsorption rate. This highlights the importance of kinetics in governing the entire adsorption efficacy of *N. pubescens* stem.

Table-2: Kinetic Equations of Various Models (non-linear)

Kinetic models	Kinetic Equation	Different parameters	Reference
Pseudo-first-order	$q_t = q_e\left(1 - e^{-k_1 t}\right)$	k_1- Pseudo-first-order rate constant(min^{-1})	[21]
Pseudo-second-order	$q_t = \frac{q_e^{\,2} K_2 t}{1 + q_e k_2 t}$	k_2 - Pseudo-second-order rate constant (g/mg/min)	[12]
Elovich	$q_t = \frac{1}{\beta}\ln\left(1 + \alpha\beta t\right)$	α - Initial rate of adsorption (mg/min) β - Desorption constant(g/mg)	[31]

q_e (mg/g)- Adsorption capability at equilibrium, q_t (mg/g) - Adsorption capability at time t, t- time

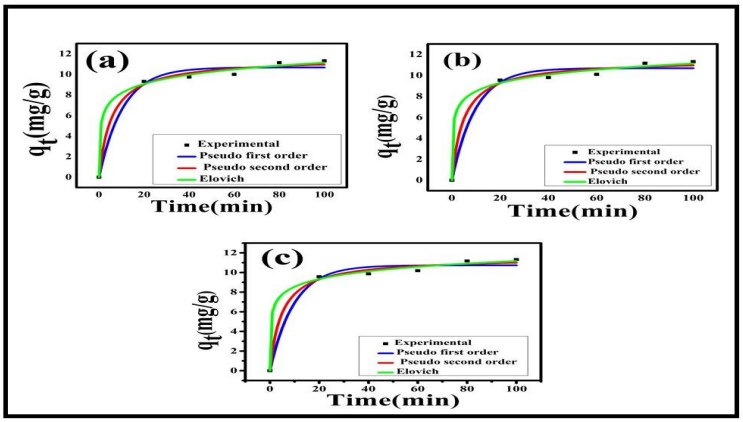

Fig.-6: Study of Kinetics Models (Pseudo first-order, Pseudo second-order, and Elovich) for the Adsorption of Lead(II) on *N. pubescens* Stem at Temperatures (a) 30℃, (b) 40℃, and (c) 50℃

Table-3: Kinetic Parameters Values for Lead(II) Ions Adsorption on *N. pubescens* Stem (25 mg/L Concentration, and pH 7) at Temperatures of (a) 30℃, (b) 40℃, and (c) 50℃

Kinetic models	Kinetic parameters	30℃	40℃	50℃
Pseudo first-order	q_e (mg/g)	10.63	10.69	10.73
	K_1(min^{-1})	0.947	0.104	0.103
	R^2	0.978	0.979	0.982
	χ^2	0.395	0.373	0.332
Pseudo second-order	q_e (mg/g)	11.57	11.48	11.52
	K_1(min^{-1})	0.0153	0.0180	0.0181

	R^2	0.988	0.989	0.991
	χ^2	0.204	0.200	0.169
Elovich	α (mg/g/min)	75.94	187.35	209.46
	β (g/mg)	0.780	0.872	0.879
	R^2	0.994	0.994	0.995
	χ^2	0.113	0.114	0.092

Study of the Isotherm of Adsorption

To know the interrelationship between the adsorbate and adsorbent at equilibrium, different non-linear isotherm models having two parameters, like the Langmuir, Freundlich, Temkin, and Toth isotherm models, have been employed at temperatures of 30℃, 40℃, and 50℃, as depicted in Fig.-7(a,b,c), respectively.[13]

Table-4: Isotherm Equations of Various Models (non-linear)

Isotherm models	Isotherm Equation	Different parameters	Reference
Langmuir	$q_e = \frac{q_m K_L C_e}{1 + K_L C_e}$	q_m - Monolayer adsorption capacity, K_L- Langmuir constant	[32]
Freundlich	$q_e = K_F C_e^{1/n}$	K_F - Freundlich constant, n-Heterogeneity factor	[31]
Temkin	$q_e = \frac{RT}{b}(lnAC_e)$	A & b - Temkin constant, R -Gas constant, T-Temperature(K)	[12]
Toth	$q_e = \frac{q_{mKC_e}}{[1 + (KC_e)^n]^{1/n}}$	q_m – Toth maximum adsorption capacity, K-Toth isotherm constant(mg/g), n-Surface heterogeneity parameter(mg/g)	[33]

Qe - Metal ion concentration on the surface of the adsorbent (mol/g), C_e - Metal ion concentration in the solution (mol/dm^3) at equilibrium.

The equations of these non-linear isotherms are exhibited in Table-4. Isotherm studies had been done with initial lead ion concentrations ranging from 25 to 100 mg/L with a biosorbent dose of 2.2 g/L at pH 7. The equations of these non-linear isotherm models are exhibited in Table-4. Various isotherm parameters of the adsorption of lead on *N. pubescens* stem are shown in Table-5. Based on the correlation coefficient (R^2), the adsorption capacity of these four isotherm models was evaluated. From Table-5, it has been shown.

Table-5: Isotherm Parameters Values for lead(II) Ions Adsorption on *N. pubescens* Stem (25 mg/L Concentration, and pH 7) at Temperatures of (a) 30℃, (b) 40℃, and (c) 50℃

Isotherm models	Isotherm parameters	30℃	40℃	50℃
Langmuir	q_m (mg/g)	42.55	42.94	50.51
	K_L(L/mg)	3.79	4.04	3.66
	R_L	0.0104	0.0098	0.0108
	R^2	0.9877	0.9864	0.9900
	χ^2	3.42	3.87	3.09
Freundlich	K_F (L/mg)	27.58	28.34	35.97
	n	0.2143	0.2273	0.3345
	R^2	0.7855	0.8258	0.8641
	χ^2	37.29	31.40	27.78
Temkin	A (L/mg)	79.40	75.046	36.72
	b	6.726	7.037	10.582
	R^2	0.9549	0.9668	0.9810
	χ^2	12.60	9.47	5.89
Toth	q_m(mg/g)	40.91	37.39	61.01
	K	4.030	4.921	2.89

	t	0.9906	0.9674	1.069
	R^2	0.9818	0.9818	0.9867
	χ^2	5.07	5.19	4.12

The value of R^2 (0.7855-0.8641) in the Freundlich model is comparatively lower than the R^2 value of the other three models (Langmuir, R^2 = 0.9864-0.9900; Temkin, R^2 = 0.9549-0.9810; and Toth, R^2 = 0.9818-0.9867). Among these models, the experimental values of Langmuir fitted perfectly to the calculated value, and its R^2 value was close to unity, and it has less chi-square value, χ^2 (3.09-3.87), than the other three models (Freundlich, χ^2 = 27.78-37.29; Temkin, χ^2 = 5.89-12.60; and Toth, χ^2 = 4.12-5.19).

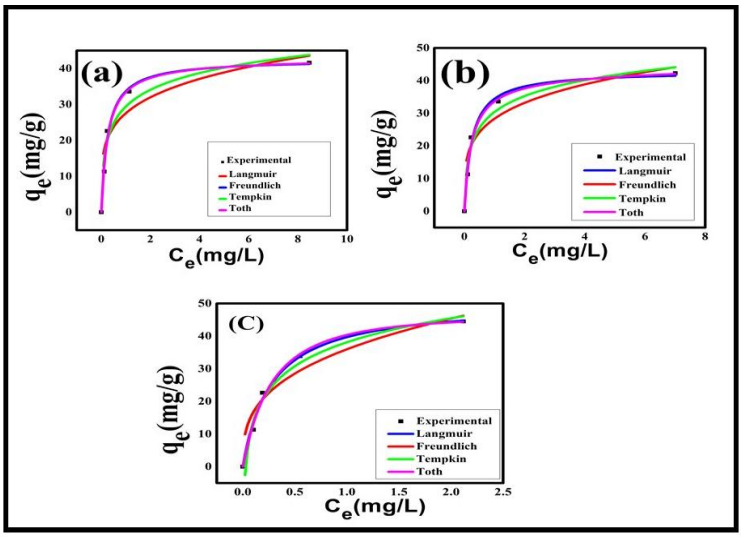

Fig.-7: Study of Isotherm Models (Langmuir, Freundlich, Temkin, and Toth) for the Adsorption of Lead(II) on *N. pubescens stem* at Temperatures (a) 30℃, (b) 40℃, and (c) 50℃

The dimensionless separation factor (R_L), which is an additional parameter in the Langmuir isotherm, might be summed up as follows:

$$R_L = \frac{1}{(1+K_L \times C_0)} \quad (3)$$

Here, the initially measured concentration of metal is denoted by C_0 (mg/g), and the Langmuir constant is represented by K_L. The isotherm could become unsuitable for $R_L > 1$, linear for $R_L = 1$, suitable for $0 < R_L < 1$, and irreversible for $R_L = 0$. To accomplish desirable biosorption, R_L must be somewhere in the range of 0 to 1. In the present study, the R_L values (0.0098-0.0108) ranged from 0 to 1, reflecting a favourable relationship between adsorbents and lead (II) in water-based solution. This points out that the adsorption of Lead(II)onto *N. pubescens* stem is encouraging.[28] The K_f values of *N. pubescens's* stem for Lead(II)ions in the Freundlich isotherm ranged from 27.58 to 35.97 in the experiment that was accomplished at various temperatures (30℃, 40℃, and 50℃). The n values for Lead(II)ions (Table-5) are worth noting since they are exceeded by 1, revealing that the adsorbate and adsorbent interacted efficiently.[39] In Temkin relation, the value of b, which denotes the heat of adsorption, increases with increasing temperature from 30℃ to 50℃, recommending that Lead(II)adsorption over the surface of the adsorbent is endothermic, and it has also been confirmed by the thermodynamic results(Table-7). Apart from that, b values at temperatures 30-50℃ are less than 80 J/mol, indicating physical adsorption at the studied temperatures.[40] Compared to the other two models, the R^2 values in the Toth isotherm are closer to the Langmuir isotherm, and for Lead(II)adsorption, the ranking of the best-fitted isotherm models is as follows:

Langmuir > Toth > Temkin > Freundlich

The better fit of Langmuir isotherm model reflects that biosorbent and Lead(II)ions in an aqueous solution are interacting favourably, and the adsorption of Lead(II)ions on the surface of the adsorbent

predominantly takes place within a monolayer along with adsorbed molecules that occupy specific positions on the surface of the adsorbent, strengthening *N. pubescens's* stem propensity to eliminate heavy metals steadily and adequately. Furthermore, Table-6 compares the potential for adsorption of the investigated adsorbent with that of various adsorbents. Based on this comparison, it can be concluded that the assessed adsorbent in the present investigation had a proficient adsorption capacity.

Table-6: Maximum Capacity of Adsorption (mg/g) for Pb(II) by different Biosorbents Found in the Literature

Adsorbent	Contact time((min)	pH	Adsorbent dose(g/L)	Concentration (mg/L)	Adsorption Capacity(mg/g)	Reference
Pistachio wood activated carbon	-	6	0.05-0.25	5.5-25	190.2	[1]
Apricot stone activated carbon	2-180	6	0.2-2	10-100	21.38	[4]
Sargassum filipendula	-	5	-	150-300	285.65	[7]
E. ferox seed coat	180	7	2	100	245.61	[10]
E. Ferox seed coat activated carbon	120	7	1.5	100	298.61	[10]
Lipia Alba	120	6	2	100	67.06	[12]
E.Rigidia activated carbon	10-90	5	0.8	50-200	279.61	[25]
Solanum melongena leaf powder (SMLP)	105	5	0.4	30-90	71.42	[26]
Moringa Olifera leaves	15-180	6	7	5-160	45.83	[30]
Oryza Sativa L.husk	-	5	0.2	50	8.6	[35]
N. pubescens stem	120	7	2.2	25-100	50.51	This study

Thermodynamic Studies on Adsorption

The study of adsorption thermodynamics was conducted using three different temperatures: 30℃, 40℃, and 50℃. Multiple variables, such as Gibbs' free energy (ΔG^o), enthalpy (ΔH^o), and entropy (ΔS^o), are employed to determine the viability of the adsorption of lead ions by the *N. pubescens* stem. The following equations are used to find out the value of Gibbs' free energy for different temperatures.

$$\Delta G^\circ = -RT\ln K_c \quad (4)$$

Table-7: Values of Different Thermodynamic Parameters for the Adsorption of Lead(II) Ions by *N. pubescens* Stem

Temperature (K)	ΔG^o (KJ mol^{-1})	ΔH^o (KJmol^{-1})	ΔS^o (KJ K^{-1} mol^{-1})
303	-11.4559	6.9084	0.06066
313	-12.1147		
323	-12.6669		

The Van't Hoff equation was used to calculate the thermodynamic variables.

$$\ln K_C = -\frac{\Delta H^\circ}{RT} + \frac{\Delta S^\circ}{R} \quad (5)$$

Where K_C Is the equilibrium constant, ΔH° Is the standard enthalpy change, ΔS° Is the standard entropy change, ΔG° Is the standard Gibbs free energy change, R It is the universal gas constant, and T is temperature (Kelvin). The plot $\ln K_C$ *vs.* T (Fig.-8) gives slope and intercept, which were used to calculate the value of ΔH° and ΔS°.[42,43] Table-7 exposes negative values of ΔG°, which indicates the adsorption process is spontaneous at all three temperatures. Besides this, the positive value of ΔH°

depicts the endothermic adsorption process, and the value of ΔS°, which is also positive, suggests that entropy increased in the adsorption process.[44,45]

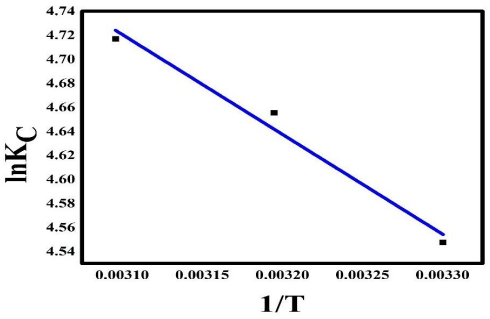

Fig.-8: Thermodynamic Study of Adsorption of Lead(II) Ions on *N. pubescens* Stem (Van't Hoff plot)

Desorption Analysis for the Reuse of the Adsorbent

Adsorbent reusability is critically important for commercial purposes and should be prioritized. This study explored the potential benefits of renewing the adsorbent material. As the number of cycles increased, the adsorbent's adsorption efficiency diminished substantially. The desorption capacity was estimated by implementing the following equation:

$$\text{Desorption capacity (\%)} = \frac{\text{The total amount of metal ions desorbed}}{\text{The total amount of metal ions adsorbed}} \times 100 \quad (6)$$

The recovery of Lead(II)from the adsorbent was 84.0, 93.5, 95.2, and 98.8% at 0.1, 0.5, 0.75, and 1 M HCl, respectively. The study found that raising the concentration of the HCl solution resulted in higher recovery percentages. Regeneration significantly impacts adsorption efficiency, with a reduction observed after the first three cycles. In acidic surroundings, H^{+} ions substitute cationic contaminants on adsorbent surfaces. The H^{+} attack combination in HCl solution causes displacement and the transformation of Pb (II) ions to chlorocompounds, making it efficacious. Due to its inexpensiveness and reusable qualities, *N. pubescens's* stem is a suitable option for the removal of Lead(II)ions from aqueous solutions.

Utilizing adsorbent made from *N. pubescens's* stem, the lead levels in aquatic solutions are considerably lowered, assisting to meet SDG-6 (Clean Water and Sanitation), particularly targets 6.3.[46.] Being an affordable and ecologically sound adsorbent, its goal is to boost the quality of the water by minimizing emissions of hazardous chemicals, limiting pollution, and eradicating waste. The concept proposes a green strategy to deal with waste by cleansing wastewater and encouraging local communities to meet global hygienic water requirements.

CONCLUSION

The Current research is concentrating on the prospect of *N. pubescens's* stem for the elimination of Lead(II)ions from sewage at a reasonable cost. The adsorption of lead ions by the stem of N. pubescens achieved equilibrium at 120 minutes at pH 7 and an adsorbent dosage of 2.2 g/L. *N. pubescens's* stem removes Pb (II) ions with a success rate of 99.8%. The porous structure of the adsorbent with functional groups and a stable charged surface is demonstrated by SEM, FTIR, and zeta potential analysis. This property aids in the binding of cationic contaminants onto the surface of *N. pubescens's* stem. Additional analysis of the equilibrium data using kinetic and isotherm models revealed details about the fundamental mechanics of the process of adsorption. The results indicated that the best match to experimental data was found using the Elovich kinetic model and the Langmuir isotherm. The Langmuir isotherm model, which has a lower chi-square and a higher R^2, provides a good explanation for the equilibrium data. The Elovich kinetic model offers a more comprehensive explanation of the kinetics used that govern the adsorption of lead ions by *N. pubescens's* stem. Adsorption is feasible, spontaneous, and endothermic, according to thermodynamic analysis. Based upon the results of the current investigations, *N. pubescens's* stem provides an economically viable substitute biosorbent for the biosorption of lead ions from effluent. Future studies might concentrate on chemical treatment of *N. pubescens's* stem to enhance its

effectiveness in adsorption and regeneration, and column adsorption will be carried out after optimizing the general behavior of the biosorbents to strengthen their performance. The current approach relies on economically viable, inexpensive tools to enhance the integrity of water that significantly supports SDG-6. In areas with limited resources, it offers an adaptable, ecologically conscious alternative for potable water and emphasizes the reutilization of locally available renewable plants.

ACKNOWLEDGMENTS

The authors thank the Department of Chemistry, Gauhati University, Guwahati, and CSIR-NEIST, Jorhat, for furnishing necessary laboratory facilities, and the Department of Chemistry, Abhayapuri College, Abhayapuri, Bongaigaon, for providing workspace to complete the work.

CONFLICT OF INTERESTS

The authors declare that there is no conflict of interest.

AUTHOR CONTRIBUTIONS

The present work is related to *SDG-6: Clean Water and Sanitation*. All the authors contributed significantly to this manuscript, participated in reviewing/editing, and approved the final draft for publication. The research profile of the authors can be verified from their ORCID ids, given below:

Karishma Talukdar http://orchid.org/0009-0008-1213-1944
Nimisha Sarma http://orchid.org/0009-0007-7707-7347
Suprakash Rabha http://orchid.org/0009-0006-9966-8319
Bhaswati Devi http://orchid.org/0000-0002-3642-0141
Manisha Goswami http://orchid.org/0009-0006-5333-951X
Emee Das http://orchid.org/0009-0007-2948-9953
Arundhuti Devi http://orchid.org/0000-0002-6593-7510

REFERENCES

1. T. P. Rangamani, M. Srinivasulu, L. B. Lakshmi, T. Srinivas, *Rasayan Journal of Chemistry*,**18(3),** 1736(2025), http://doi.org/10.31788/RJC.2025.1839337
2. P. Miretzky, A.F. Cirelli, *Journal of Hazardous Materials*, **180**, 1(2010), https://doi.org/10.1016/j.jhazmat.2010.04.060
3. Q. Wang, Y. Yang, Z. Yang, W. Han, L. Yuan, L. Zhang, X. Huang, C*hemical Engineering Journal Advances*, **11**, 1(2022), https://doi.org/10.1016/j.ceja.2022.100295
4. H. Medhi, P.R. Chowdhury, P.D. Baruah, K.G. Bhattacharyya, *American Chemical Society Omega*, **5**, 13489(2020), https://dx.doi.org/10.1021/acsomega.9b04032
5. F.O. Afolabi, P. Musonge, B.F. Bakare, *Cogent Engineering*, **8**, 1(2021), https://doi.org/10.1080/23311916.2021.1886730
6. L. Mouni, D. Merabet, A. Bouzaza, L. Belkhiri, *Desalination,* **276**,148(2011), https://doi.org/10.1016/j.desal.2011.03.038
7. Y. Ge, Z. Li, *ACS Sustainable Chemistry & Engineering,* **6**, 7181(2018), https://doi.org/10.1021/acssuschemeng.8b01345
8. A.R. Iftikhar, H.N. Bhatti, M.A. Hanif, R. Nadeem, *Journal of Hazardous Materials*, **161**,941(2009), https://doi.org/10.1016/j.jhazmat.2008.04.040
9. A. Verma, S. Kumar, S. Kumar, *Journal of Environmental Chemical Engineering*, **4**,4587(2016), https://doi.org/10.1016/j.jece.2016.10.026
10. S. Kalita, M. Pathak, G. Devi, H.P. Sarma, K.G. Bhattacharyya, A. Sarma, A. Devi, *Royal Society of Chemistry Advances,* **7**,27248 (2017), https://doi.org/10.1039/C7RA03014B

11. H. Grabi, A. Ouakouak, S. Kadouche, W. Lemlikchi, F. Derridj, A.T. Mohddin, *Surfaces and Interfaces*,**30**, 101947(2022), https://doi.org/10.1016/j.surfin.2022.101947
12. B. Devi, M. Goswami, S. Rabha, S. Kalita, H.P. Sarma, A. Devi, *American Chemical Society Omega*, **8,** 15141(2023), https://doi.org/10.1021/acsomega.3c00142
13. S. Kumar, S. Narayanasamy, R.P. Venkatesh, *Separation Science and Technology,* **54**,2783(2018), https://doi.org/10.1080/01496395.2018.1560333
14. S. Rabha, B. Devi, M. Goswami, E. Das, N. Sarma, A. Devi, *Chemistry Select*, **8**,1(2023), https://doi.org/10.1002/slct.202302149
15. R.I.R. Blyth, H. Buqa, F.P. Netzer, M.G. Ramsey, J.O. Besenhard, P. Golob, M. Winter, *Applied Surface Science*, **167**, 99(2000), https://doi.org/10.1016/S0169-4332(00)00525-0
16. A. Ashraf, S.A. Dastgheib, G. Mensing, M.A. Shannon, *The Journal of Supercritical Fluids*, **76**, 32(2013), http://dx.doi.org/10.1016/j.supflu.2013.01.017
17. R. Al-Gaashani, A. Najjar, Y. Zakaria, S. Mansour, M.A. Atieh, *Ceramics International*,**45**, 14439(2019), https://doi.org/10.1016/J.CERAMINT.2019.04.165
18. X. Chen, X. Wang, D. Fang, *Fullerenes, Nanotubes and Carbon Nanostructures*, **28**,1048(2020), http://dx.doi.org/10.1080/1536383X.2020.1794851
19. F. Wang, X. Lu, X.-Y. Li, *Journal of Hazardous Materials,* **308**,75(2016), https://doi.org/10.1016/j.jhazmat.2016.01.021
20. J. Zhao, M.N. Rafat, C.-M. Yoon, Oh. W.-C., *Nanomaterials,* **12**,1(2022), https://doi.org/10.3390/nano12203639
21. R.J.J. Jansen, H. van. Bekkum, *Carbon,* **33**, 1021(1995), https://doi.org/10.1016/0008-6223(95)00030-H
22. M. Ayiania, M. Smith, A.J.R. Hensley, L. Scudiero, J.-S. McEwen, M. Garcia-Perez, *Carbon*, **162**, 528(2020), https://doi.org/10.1016/j.carbon.2020.02.065
23. E. Das, S. Rabha, K. Talukdar, M. Goswami, A. Devi, *Environmental Monitoring and Assessment*, **195**,1(2023), https://doi.org/10.1007/s10661-023-11656-1
24. S. Mahiya, S.K. Sharma, G. Lofrano, *Cogent Environmental Science*, **2**,1(2016), http://dx.doi.org/10.1080/23311843.2016.1218993
25. A.Q. Alorabi, F.A. Alharthi, M. Azizi, N. Al-Zaqri, A. El-Marghany, K.A. Abdelshafeek, *Applied Sciences,***10**, 1(2020), https://doi.org/10.3390/app10217450
26. S.O. Owalude, A.C. Tella, *Beni-Suef University Journal of Basic and Applied Sciences,* **5**,377(2016), https://doi.org/10.1016/j.bjbas.2016.11.005
27. O. Gerçel, H.F. Gerçel, *Chemical Engineering Journal,* **132**, 289(2007), https://doi.org/10.1016/j.cej.2007.01.010
28. G. Yuvaraja, N. Krishnaiah, M.V. Subbaiah, A. Krishnaiah, *Colloids and Surfaces B: Biointerfaces*, **114**,75(2014), https://doi.org/10.1016/j.colsurfb.2013.09.039
29. H. Pahlavanzadeh, M. Motamedi, *Journal of Chemical & Engineering Data,* **65,**185(2020), https://doi.org/10.1016/j.jenvman.2019.01.087
30. L.M. Zacaroni, Z.M. Magriotis, M.D.G. Cardosa, W.D. Santiago, J.G. Mendonca, S.S. Vieira, D.L. Nelson, *Food Control*, **47**,536(2015), https://doi.org/10.1016/j.foodcont.2014.07.035
31. S. Kumar, T. Shahnaz, N. Selvaraju, P.V. Rajaraman, *Environmental Monitoring and Assessment*, **192**, 1(2020), https://doi.org/10.1007/s10661-020-8181-x
32. M. Goswami, B. Devi, E. Das, S. Rabha, H.P. Sarma, A Devi, *Environmental Monitoring and Assessment,***196**,1(2024), https://doi.org/10.1007/s10661-024-12617-y
33. S.-A. Sajjadi, A. Meknati, E.C. Lima, G.L. Dotto, D.I. Mendoza-Castillo, I. Anastopoulos, F. Alakhras, E.I. Unuabonah, P. Singh, A. Hosseini-Bandegharaei, *Journal of Environmental Management,* **236,** 34(2019), https://doi.org/10.1016/j.jenvman.2019.01.087
34. M. Imran, K. Anwar, M. Akram, G.M. Shah, I. Ahmad, N.S. Shah, Z.U.H. Khan, M.I. Rashid, M.N. Akhtar, S. Ahmad, M.Nawaz, & R.J. Schotting, *International Journal of Phytoremediation,***21**,777(2019), https://doi.org/10.1080/15226514.2019.1566880
35. M. Varnaseri, Z.M. Zadeh, F. Abdolmohammad, F. Zisti, D. Balarak, M.K. Saloot, *Water Conservation Science and Engineering*, **9**, 1(2024), https://doi.org/10.1007/s41101-024-00279-3

36. E. Bazrafshan, M.Sobhanikia, F.K. Mostafapour, H.Kamani, D. Balarak, *Global NEST Journal*, **19**,269(2017), https://doi.org/10.30955/gnj.001708
37. U.A. Edet, A.O. Ifelebuegu, *Processes*, **8**, 1(2020), https://doi.org/10.3390/pr8060665
38. N. Ayawei, A.N. Ebelegi, D. Wankasi, *Journal of Chemistry,* **2017**,1(2017), https://doi.org/10.1155/2017/3039817
39. S. Raghav, D. Kumar, *Journal of Chemical & Engineering Data*, **63**,1682(2018), https://doi.org/10.1021/acs.jced.8b00024
40. A.A. Alameri, R.H.C. Alfilh, S.A. Awad, G.S. Zaman, T.J. Al-Musawi, M.M. Joybari, D. Balarak, G. McKay, *Biomass Conversion and Biorefinery*, **14**, 27001(2022), https://doi.org/10.1007/s13399-022-03372-6
41. M.M.D. Zulkali, A.L. Ahmad, N.H. Norulakmal, *Biosource Technology,* **97**,21(2006),https://doi.org/10.1016/j.biortech.2005.02.007
42. S. Pu, Y. Hou, C. Yan, H. Ma, H. Huang, Q. Shi, S. Mandal, Z. Diao, W. Chu, *ACS Sustainable Chemistry & Engineering*, **6**, 16754(2018), https://doi.org/10.1021/acssuschemeng.8b04028
43. J.R.R. Prathipati, T. Rambabu, R. Kota, S. Ampolu, S. B. Matcha, P. V. S. K. P. Varma, N. Taidala, T. Narasimhulu, *Rasayan Journal of Chemistry*, **18**,1541(2025), http://doi.org/10.31788/RJC.2025.1839148
44. M. M.-Hassan, M. Yasin, M. Yousra, R. Ahmad, S. Sarwar, *Environmental Science and Pollution Research*, **25**, 12570(2018), https://doi.org/10.1007/s11356-018-1300-3
45. G. Saraswathi, M. Vasuki, *Rasayan Journal of Chemistry*, **18**,1431(2025), http://doi.org/10.31788/RJC.2025.1839294
46. M. Napitupulu, P. Ningsih, T. Santoso, D.K. Walanda, *Rasayan Journal of Chemistry*, **18**,1654(2025), http://doi.org/10.31788/RJC.2025.1839361

[RJC-9404/2025]